Environmental Earth Sciences (2023) 82:496
https://doi.org/10.1007/s12665-023-11163-z

ORIGINAL ARTICLE

Assessing mesoscale permeability in unsaturated, fractured, and karstified carbonate reservoirs: a joint geological, petrophysical, and hydraulic approach for the interpretation of injection tests

Charles Danquigny[1,2] · J. Coqueret[1] · G. Massonnat[1] · P. Léonide[3] · M. Barbier[4] · L. Dal Soglio[4] · J. L. Lesueur[1]

Received: 14 April 2023 / Accepted: 2 September 2023 / Published online: 26 September 2023

Abstract

In the study of subsurface reservoirs, permeability is a key parameter whose evaluation and extrapolation at the desired scale, such as that of the numerical model mesh, are both a necessity and a difficult task. Relating permeability measurements to the geological characteristics of the rock, at intermediate scales seldom characterized, can help understanding the heterogeneity of the medium and correctly determining the permeability at the desired scale. This concern is particularly important in karst reservoirs, which exhibit highly variable permeability at different scales of observation and from one location to another. Here, we study the petrophysical and geological properties of carbonate facies from the centimeter to the meter scale. Several boreholes a few meters apart were cored and exhaustively described. Petrophysical measurements were made on rock samples, while inter-packer injection tests were undertaken to investigate some meter intervals of the medium surrounding the wells. The results show that the investigated medium is a complex multi-medium with a multi-scale heterogeneity. The detailed geological description allowed explaining the differences between the permeability values at different scales and from one interval to another. Relationships were quantified between the texture of the limestone matrix, the density and aperture of the discontinuities, the permeability of the matrix, and the permeability contrast related to the dual medium at the meter scale. A strong correlation between this permeability contrast and the aperture of the discontinuities, itself more correlated to the texture of the rock than to the facies, is highlighted.

Keywords Karst · Permeability · Scale · Matrix · Fracture · Hydraulic tests

Introduction

Although permeability is a key parameter for the study of flow in subsurface reservoirs (e.g., groundwater, hydrocarbon, or CO_2 storage), it can only be assessed by indirect measurements, mainly based on the pressure–discharge relationship, and rarely at the desired scale. Indeed, laboratory measurements can hardly exceed the cubic decimeter, and well tests or springs hydrographs investigate large volumes, possibly several thousand even millions cubic meters, that are difficult to delimit and constrain, making it equally difficult to link the interpreted permeability to the physical properties of the medium. Between these two end-members, the poorly characterized meter to hectometer scale is also the scale of the mesh of numerical models usually applied to understand and predict the dynamics of subsurface reservoirs. When hydraulic tests, nevertheless, target small volumes, they are tricky to interpret: the volume investigated and its geometry are uncertain, the assumptions associated with the analytical solutions conventionally used for interpretation may not be met, and in general, the results depend largely on the location of the measurement relative to the highly permeable elements, such as karst conduits for example (Jazayeri Noushabadi et al. 2011; Maréchal et al. 2014; Marechal et al. 2008).

This twofold problem of indirect measurement at an inappropriate scale makes it necessary but also difficult, due to

✉ Charles Danquigny
charles.danquigny@univ-avignon.fr

1 TotalEnergies, Centre Scientifique et Technique Jean Féger (CSTJF), Pau 64000, France

2 UMR EMMAH, Avignon Université, 301 Rue Baruch de Spinoza, 84916 Avignon, France

3 CEREGE UM 34, CNRS, IRD, Aix-Marseille Université, 3 Place Victor Hugo, 13331 Marseille, France

4 Akkodis, 4 Rue Jules Ferry, 64000 Pau, France

the lack of consistent data, to deal with permeability scaling issues. The scarcity of data and the lack of measurements at different scales often leads to erroneous extrapolations of the properties measured in wells. Furthermore, extrapolating measurements and filling flow simulation grids with properties often poorly or inefficiently integrate geological constraints that would make the model more robust and closer to reality (Brunetti et al. 2019; Enemark et al. 2019; Linde et al. 2017, 2015).

This is a particularly relevant concern in karst reservoirs, where hydraulic conductivity largely depends on the observation scale and can impressively vary from one place to another (Hartmann et al. 2014; Jazayeri Noushabadi et al. 2011; Medici and West 2021). Indeed, fractures and karst conduits add heterogeneity to the medium. This heterogeneity is both localized and contrasted, respectively, due to the discrete nature (two-dimensional and one-dimensional elements in a three-dimensional medium) and the filling or, more often, the lack of filling of these features. These discontinuities, often numerous and varied, give the karst its specificity in terms of reservoir properties. In most cases, they are highly conductive (Ford and Williams 2007). The representation of the most conductive elements, and with it the overall hydraulic conductivity of the studied medium, increases with the scale of observation (Galvao et al. 2016; Hartmann et al. 2014). The network structure and connectivity of both fractures and conduits can also considerably increase the size or even question the existence of a representative elementary volume of the medium, i.e., a scale at which equivalent homogeneous properties such as permeability can be defined. They induce complex dynamic responses, difficult to characterize and to reproduce numerically.

The difficult discrete representation of the multi-scale heterogeneity of fractured-karstified carbonates often hamper simulation of flow physics in these media. Physically based gridded flow models, which are useful management tools (understanding, forecasting) usually applied to simple aquifers, are rarely applied to karst aquifers (Ghasemizadeh et al. 2012; Hartmann et al. 2014). Indeed, such models raise the particularly delicate question in karst environment of the homogenization of properties at the mesh scale and that of taking into account the networks of fractures and karst conduits and their flow physics. Addressing such questions requires multi-scale characterization of the permeability field (Galvao et al. 2016; Halihan et al. 1999; Massonnat et al. 2019).

This study is part of a wider research project (Danquigny et al. 2019b; Massonnat et al. 2017) dedicated to the understanding and modeling of fluid dynamics at various scales of a vast karstified carbonate aquifer, namely the Fontaine-de-Vaucluse aquifer (southeastern France), with respect to its multiphase geological history. Here, we are interested in the characterization of the permeability of different carbonate rock-types from centimeter to meter scale and the relation with their geological characteristics (facies, texture, and structural features). To this end, this work makes use of different disciplinary studies carried out on a well-constrained experimental area comprising several boreholes to establish a coupled and interdisciplinary analysis.

Based on a robust facies model (Michel et al. 2023; Tendil et al. 2018), Danquigny et al. (2019a) quantified the high intra- and inter-facies variability of petrophysical properties measured at small scales for the geological formation of interest, namely the Urgonian of southeastern France. Then, Cochard (2018) focused on the boreholes cored in the experimental area and revealed the complex heterogeneity of the rock at various scales, the result of an equally complex geological history involving sedimentary, diagenetic (including karst genesis) and tectonic processes. Petrophysical measurements were performed on rock samples, so-called plugs, taken from the cores, while water injection tests between packers were used to investigate some meter intervals of the medium surrounding the wells.

The different porosity types (primary matrix, secondary fractures, and tertiary karst features) have physical characteristics, and hence a relative influence on hydraulic conductivity, which vary with the scale of observation. Even with a good knowledge of the geological setting and facies, both these characteristics and their relative weighting according to the scale are difficult to characterize and deconvolute. It is therefore particularly difficult in such a context to scale up permeability for modeling. In this paper, we use the detailed geological description of the tested intervals and a thorough interpretation of the hydraulic tests to further characterize these relationships and provide a coupled analysis that has not been done before.

Moreover, due to the location in the unsaturated zone of the aquifer and the low matrix permeability of the studied rocks, performed hydraulic tests have two particularities: (i) they are "constant-head tests" or "constant pressure injection tests", i.e., water is injected at a constant pressure, while the decline of the injection rate is studied, (ii) the initial saturation of the medium surrounding the well is poorly known, varies in space and time, and is affected by the experiment. This configuration raises questions concerning the interpretation of the tests. To address these issues, in the absence of an analytical solution fully adapted to the unsaturated medium, we have tested and confronted the analytical solutions assuming the saturated medium and a numerical approach assuming the unsaturated medium. Results are faced to the small-scale measurements and to the geological description of the tested intervals.

Materials and methods

The experimental site

Global context: the Fontaine-de-Vaucluse aquifer and the Urgonian Formation (South-Eastern France)

The Fontaine-de-Vaucluse aquifer is a very well-known karst system, notably for its spring, which gave its name to the class of Vauclusian springs, formed by water running upwards from a main conduit deeper than the base water level (Blavoux et al. 1992; Ford and Williams 2007). Its catchment area covers more than 1000 km^2 and converges toward a main outlet, the so-called Fontaine de Vaucluse (Fig. 1A), whose average flow rate is around 20 m^3/s (Bonacci 2007; Cognard-Plancq et al. 2006). Numerous hydrogeological studies have therefore investigated this aquifer, in particular the dynamic behavior of its outlet and its unsaturated zone, whose average thickness is around 700 m (e.g., Blondel et al. 2012; Carriere et al. 2016; Emblanch et al. 2003; Fleury et al. 2007; Ollivier et al. 2019).

This water body develops in a carbonate series, which can reach 1500 m thickness, from the Valanginian marls to the marls of the upper Aptian (Blavoux et al. 1992). The series includes the Urgonian formations, Barremo-Aptian in age. The latter has widely been studied for several decades by geologists, who described the sedimentary depositional system (e.g., Barbier et al. 2021; Borgomano et al. 2013; Leonide et al. 2012, 2014; Masse 1976, 1967; Michel et al. 2023; Tendil et al. 2018).

Despite a good knowledge of the aquifer dynamics and early attempts to apply physically based gridded flow models (Bonnet et al. 1976), the high heterogeneity and complexity of the system, as well as the lack of spatialized data, have led to the preferential application of lumped models (Fleury et al. 2007; Mazzilli et al. 2019; Ollivier et al. 2020), as for many karst systems (Hartmann et al. 2014). However, recent advances in the knowledge of spatial distribution of depositional environments and facies (Barbier et al. 2021; Tendil et al. 2018) in the one hand, and fractures and karst networks genesis (Dal Soglio et al. 2019) on the other hand make it possible to consider the application of gridded flow models. For this, the characterization of petrophysical properties of the different types of rock at different scales is a necessary next step.

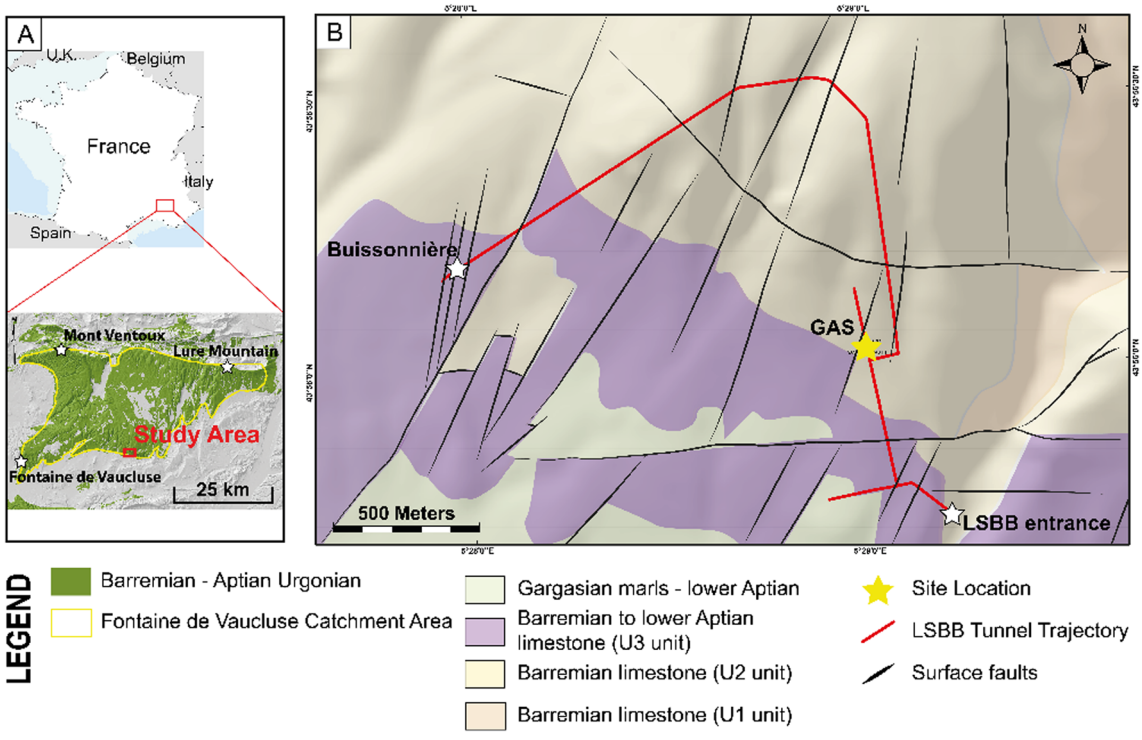

Fig. 1 Location and geological context of the study site (GAS area, in LSBB Underground Research Laboratory, in Fontaine-de-Vaucluse catchment area)

The experimental site: the GAS borehole platform at the LSBB underground laboratory

In the south of the Fontaine-de-Vaucluse catchment area, the LSBB (Laboratoire Souterrain à Bas Bruit–Low Noise Underground Research Laboratory) is an underground research laboratory giving access to the carbonate rock along a 3.8 km-long tunnel. This tunnel is almost horizontal and reaches a depth of 519 m under the top of the mountain it crosses (Fig. 1B). The laboratory offers a unique, interdisciplinary experimental setting. In particular, it is a suited site for coupling geological, geophysical, and hydraulic characterizations of carbonate reservoirs (Danquigny et al. 2021, and references therein). Among other facilities, five boreholes, called from P1 to P5, were cored at a 280 m depth, in the so-called GAS area (Gallery Against Shockwave–Figs. 1B, 2). They are spaced by a few meters only and have an average depth of 21 m (Fig. 2).

Cochard (2018) precisely described the cores and panoramic 360° imagery log of these five boreholes to establish both lithostratigraphic logs and a comprehensive reporting of the discontinuities affecting the reservoir. A vertical cross-section has been established from the description of the boreholes logs and the GAS tunnel's wall (Fig. 2). Two main carbonate facies associations belonging to the stratigraphic unit Urgonian 2 (U2) are present in the GAS area: the fine peloid–foraminiferal facies FA2, with texture ranging from mudstone to grainstone, and the rudists-dominated facies FA3, with texture ranging from packstone to floatstone.

186 rock samples were also taken from the P2 cores to perform petrophysical measurements. These samples, or plugs, have standard dimensions of 2 inches in height and 1 inch in diameter, i.e., a volume of about 25 cm^3 (Fig. 4). Their location was chosen to sample a volume of rock which is both homogeneous and as representative of the type of rock as possible. As a consequence, where discontinuities or fossils larger than the plug volume were present, they were deliberately avoided during sampling (e.g., Fig. 4). Porosity was measured on all samples. Values range from 1 to 21%, with an average value of 9% and a standard deviation of 6%. Porosity values are greater for the rudist-rich facies FA3 (10% on average) than for the peloid–foraminiferal facies FA2 (3% on average). Permeability was measured on

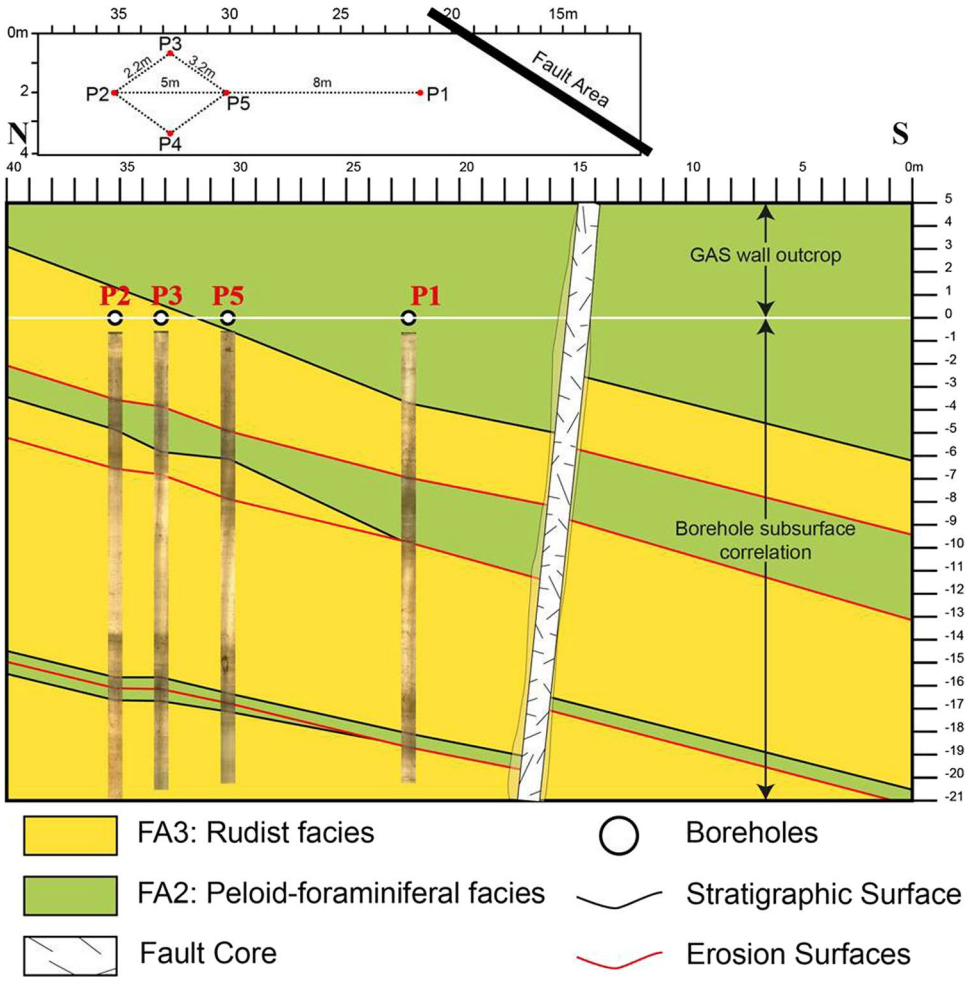

Fig. 2 Map of the GAS boreholes platform and corresponding vertical cross-section showing facies associations along the GAS tunnel wall and correlations projected from four boreholes (after Cochard et al. 2020, modified)

47 samples. The low limit of quantification (0.01 mD) was reached for 24 of them. Highest values, up to 3.54 mD (1 mD = 10^{-15} m^2, which is equivalent to a hydraulic conductivity for a water-saturated medium of 10^{-8} m/s), are obtained for the rudist-rich facies FA3. Values are reported in Fig. 6.

Here, the term discontinuity refers generically to any discrete feature, such as joints, veins, styloliths, and karst, as opposed to the matrix it affects. In the experimental area, two intervals appear to be intensely affected by discontinuities and present numerous fractures, karst features, or stylolites. On the well P2 for instance, these intervals are located at 4–6 m depth, with poorly opened discontinuities (stylolites and joints), and at 16–19 m depth, with evidence of karstification and very open discontinuities (Figs. 3, 4e, f). Therefore, in these intervals, the matrix having a low-permeability, fluid flow is very likely to be controlled by the conductive discontinuities.

The reader can refer to the work of Cochard (2018) and Cochard et al. (2020, 2021) for more details about these cores' description and small-scale petrophysical measurements. The results used in this study are synthetized in Fig. 3.

The diameter of the boreholes is furthermore large enough to allow hydraulic tests to be performed on packer-sealed intervals. Thus, these wells offer an excellent opportunity to study the relationships between lithology, discontinuities, and petrophysical properties at different scales.

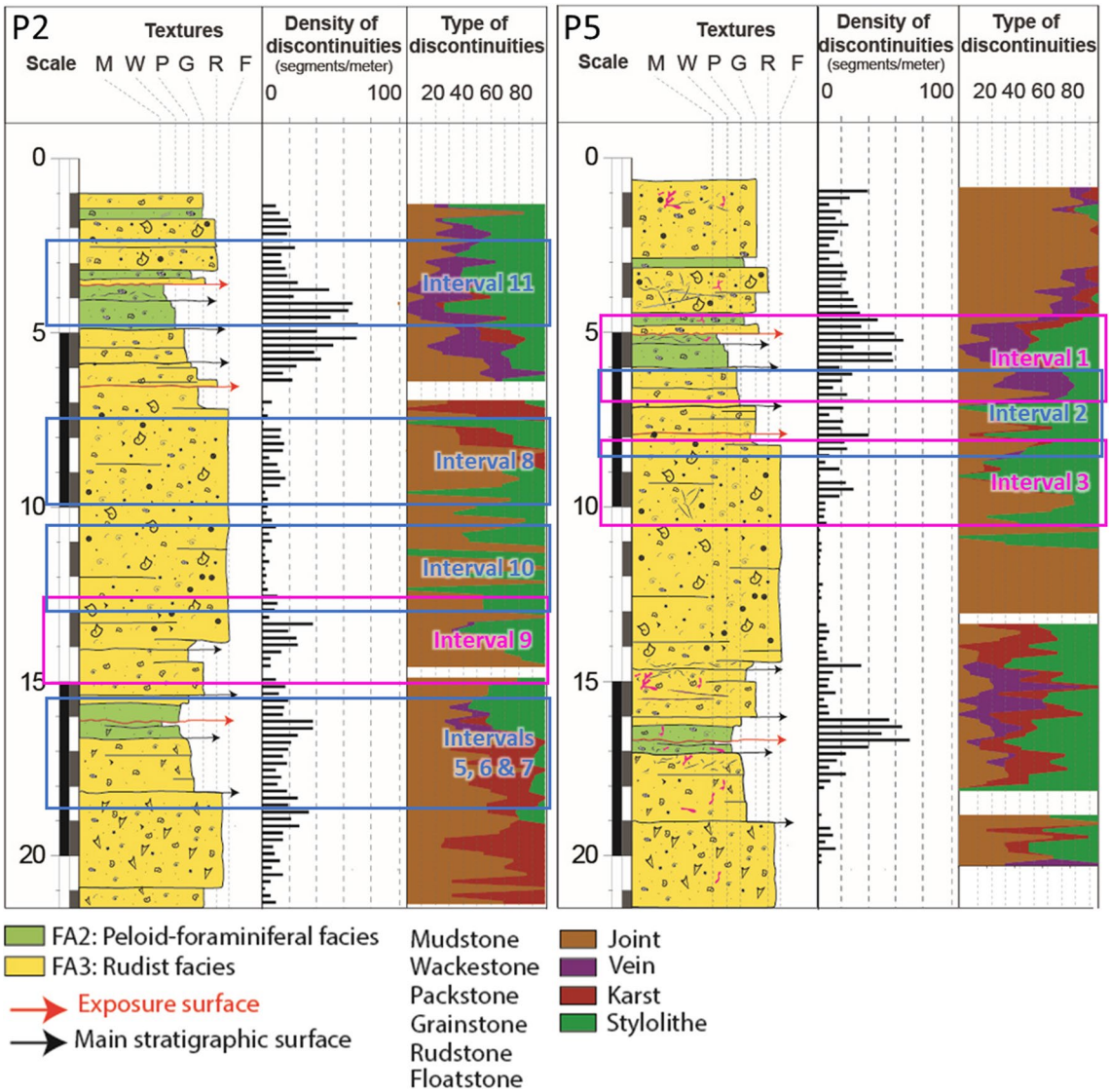

Fig. 3 Geological description of the boreholes with location of the tested intervals (after Cochard et al. (2020), modified)

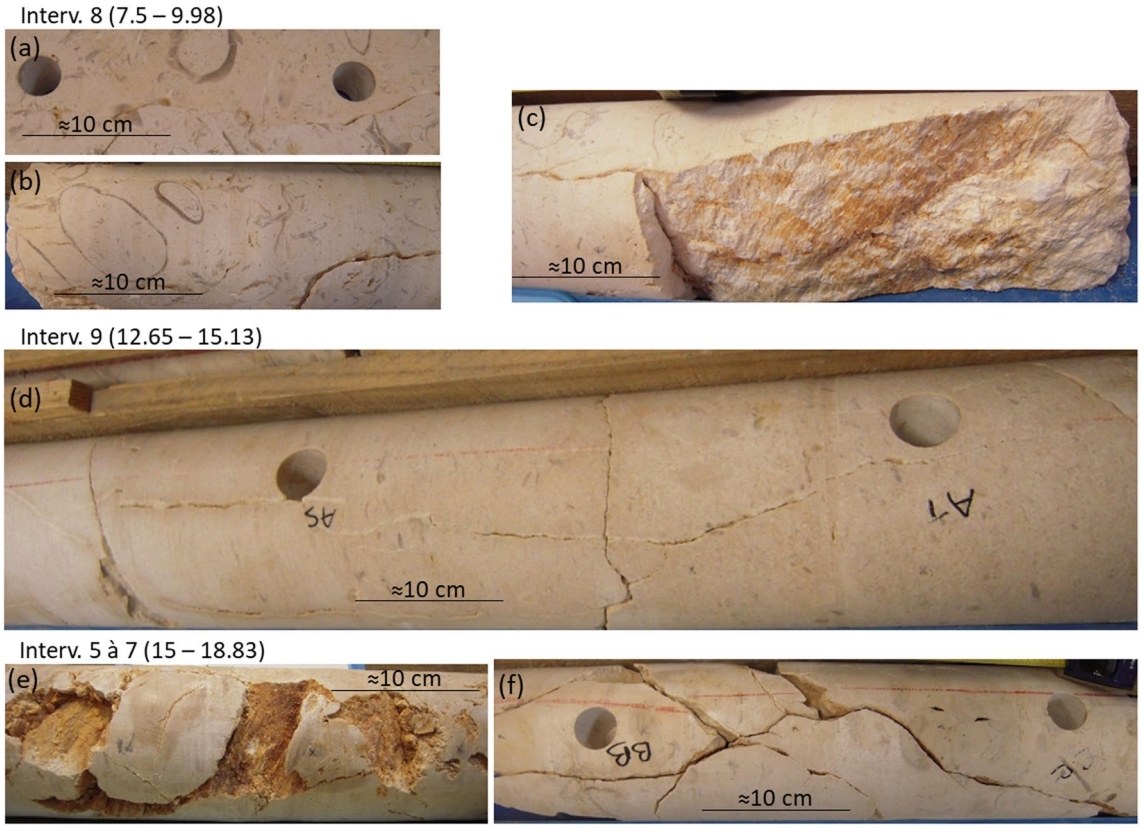

Fig. 4 Pictures of the cores from the P2 borehole illustrating both the heterogeneity of the intervals 5–9 targeted by hydraulic tests and some volumes sampled for small-scale petrophysical measurements

Description of the tested intervals

Ten intervals of 2.48 m thickness were selected for hydraulic testing: three intervals in the P5 borehole numbered from 1 to 3, and seven intervals in the P2 borehole numbered from 5 to 11, number 4 having been discarded for lack of conclusive measurements. The intervals 5 (from 15.65 to 18.13 m), 6 (from 16.35 to 18.83 m), and 7 (from 15 to 17.48 m) overlap and are therefore treated together in this study. While considering experimental constraints, all these intervals were selected to test different distributions of both facies, textures, and discontinuities. The discontinuities in each interval were characterized by their maximum aperture reported by Cochard (2018) and Duboeuf (2018). Figures 3 and 7 illustrate the diversity of the tested intervals.

Intervals 1, 5–7, and 11 investigate the two facies with different proportions, while others investigate only the rudist facies, which is the most represented in the study site. The intervals 3, 8, and 10 mostly consist of floatstone (> 96%), with cemented fossils a few centimeters thick (up to decimeter in places; Fig. 4a, b) and very few poorly open (< 1.5 mm) discontinuities. Notably, the neighboring intervals 8 and 10 are composed of one and the same rock type (rudist-rich floatstone) and differ in their density of discontinuities, which is almost zero for interval 10. In contrast, intervals 1, 5–7 and 11 correspond to the most fractured and karstified limestone and the finest textures. They present multi-millimeter voids and the aperture of the discontinuities can reach 8–10 mm, in particular for intervals 5–7 (Fig. 4e, f).

Hydraulic tests

Measurements' protocol

Constant-head tests (or constant-pressure tests) consist in keeping pressure or water level constant while injecting or pumping water into the aquifer and recording flowrate. Performed less frequently than the other methods (e.g., pumping and slug tests), these tests are more suitable to low-permeability formations for two main reasons. First, keeping a pressure constant while injecting or pumping water in an aquifer is technically easier than keeping a constant rate in a low-permeability formation (Mejias et al. 2009; Renard 2005). Therefore, data acquired from the tests are of a better quality. Second, the pressure being constant in the well, wellbore storage effects are much-reduced (Doe 1991; Renard 2005).

In the case of this study, injection tests were performed on each interval sealed by inflatable packers. This system allows the isolation of sealed-off targeted sections by inflating packers with under-pressured azote. A probe, located between the packers, measures the pressure in the isolated interval. A pump located at surface controls the injection of water in the chamber and an electromagnetic flowmeter measures the flowrate at surface. Both the pump and the flowmeter are directly linked to an acquisition station which allows the regulation of the flowrates (or the pressure) thanks to a control gauge.

Several types of tests were performed on each interval, including slug tests, injection by pressure steps, and constant-head tests. The whole campaign and all the tests carried out are presented in the work of Duboeuf (2018), Duboeuf et al. (2017) and Duboeuf et al. (2021). Cochard (2018) provided a first estimation of hydraulic conductivity from some of these tests. We synthetized these rough estimates in a previous paper, highlighting both differences and no evident correlation between the measurements at different scales (Danquigny et al. 2019a). Then, a selection of 28 good quality constant-head tests and constant-pressure steps from this campaign was further interpreted and simulated (Danquigny et al. 2023). Here, the permeability values resulting from the interpretation of these 28 selected tests are analyzed in detail with respect to small-scale measurements and the fine geological characteristics of the rocks tested. The selected tests are summarized in Table 1.

During a previous campaign of hydraulic testing eight intervals of 1 m thickness were tested (five pulse tests and three constant-flow-rate injections) in the P2 borehole. This campaign did not aim directly petrophysical measurements but Jeanne et al. (2013) provided nevertheless some estimations of these properties from numerical simulations. These are also considered but not reinterpreted in this study (Fig. 6).

Analytical interpretation methods

The analytical interpretation of hydraulic tests consists of fitting a mathematical solution to the measurements to determine the properties of the investigated medium, in particular its permeability. As with the other hydraulic testing methods, constant-pressure injection tests can be interpreted using type-curve matching. However, the pressure being constant, usual analytical models cannot be applied.

The first transient rate analysis for constant-pressure injection tests was developed by Jacob and Lohman (1952). This traditional method assumes a cylindrical radial flow into a fully saturated, infinite, isotropic, and homogeneous reservoir (Doe 1991; Jacob and Lohman 1952; Renard 2005). This model was refined by Hantush (1959) who added the effect of possible leakage and flow boundaries in the model. The classical approach was to plot the rate versus time or log(time) and to fit the Jacob & Lohman type-curve to estimate hydraulic properties. However, this approach makes serious assumptions and might oversimplify the flow in the formation. Indeed, in case of a more complex aquifer, the actual flow might not be purely radial, and thus, the model does not realistically represent flow in the reservoir. This can lead to gross or erroneous estimations of the hydraulic properties of the aquifers (Ferroud et al. 2019).

Two major developments have improved the interpretation of these tests. First, the derivative analysis approach (Bourdet et al. 1983; Renard et al. 2009) was extended for constant-pressure tests by plotting the derivative of the inverse flow rate (Doe 1991; Geier et al. 1996). Subtle changes in the aquifer conditions are much more visible than on a classical "Rate vs. time" plot. Therefore,

Table 1 Summary of hydraulic constant-head tests (CHT) and constant-pressure steps (PAL) interpreted

Interval	1	1	3	3	3	3	5	6	7	7	8	8	8	8
Test	PAL 1	PAL 2	CHT 1	CHT 2	CHT 3	CHT 4	PAL 2	PAL 2	PAL 1	PAL 3	CHT 1	CHT 2	CHT 3	PAL 5
Pres. (bars)	1	2.7	43	47	43	44	5	8	3	8	53	54	45	29
Dur. (s)	95	80	600	1100	1100	2050	44	40	55	30	240	180	1320	70
Kco (mD)	307	312	12.9	13.7	12.7	16.2	186	126	126	121	14.9	10.4	14.4	14.3
Kca (mD)	0.0009	0.0007	0.292	0.222	0.208	0.252	0.005	0.005	0.007	0.005	1.98	1.87	1.31	1.5
Interval	2	2	2	9	9	9	9	10	10	10	10	11	11	11
Test	CHT 1	PAL 2	PAL 3	CHT 1	CHT 2	CHT 3	PAL 1	CHT 1	CHT 2	CHT 3	CHT 4	CHT 1	PAL 9	PAL 15
Pres. (bars)	43	2.5	8	53	52	48	15	50	54	59	48	58	48	35
Dur. (s)	210	120	250	107	137	948	90	90	60	50	470	131	60	70
Kco (mD)	29.8	22.9	42.8	10.9	13.1	14.6	11.1	1.90	3.09	3.38	6.04	6.57	3.00	3.07
Kca (mD)	0.0627	0.0843	0.578	0.04	0.04	0.04	0.04	0.91	0.99	0.89	0.84	0.002	0.002	0.002

Pres. Pressure, *Dur.* duration, *Kco* permeability of the conductive medium from analytical interpretation, *Kca* permeability of the capacitive medium from analytical interpretation

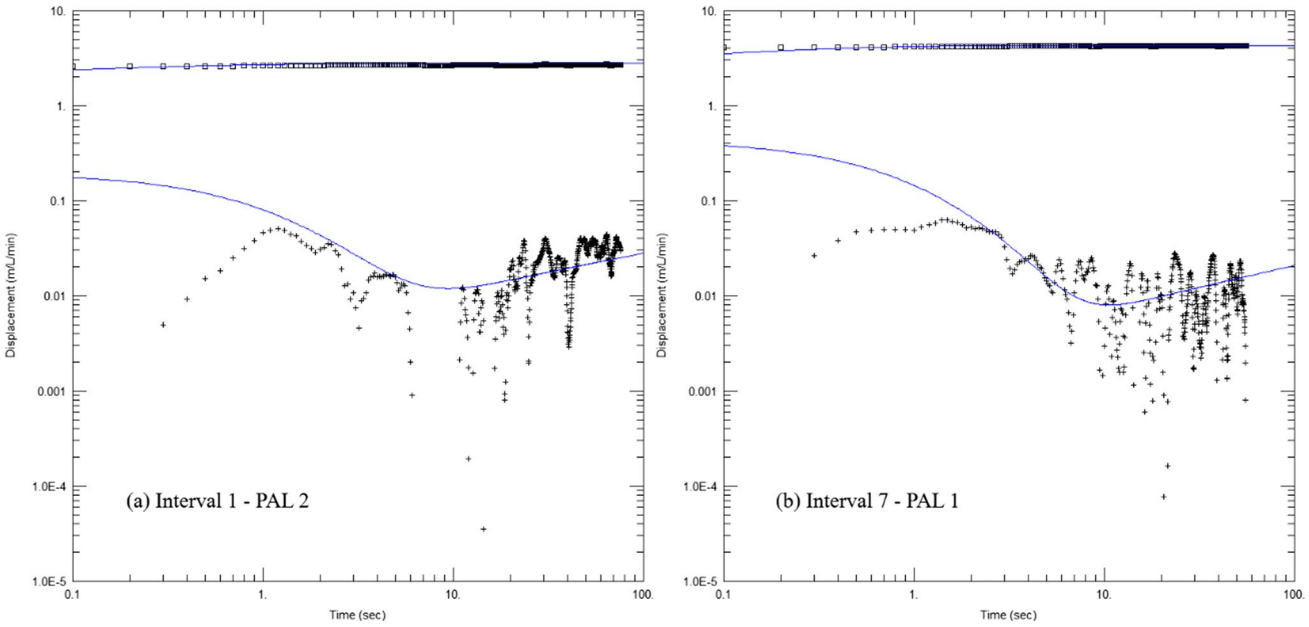

Fig. 5 Examples of diagnostic plots of injection tests showing both the displacement, i.e., inverse flow rate divided by the pressure (black squares), and the derivative (black crosses), which U-shape is typical of a dual-medium behavior, and the fitted corresponding Barker solution (blue lines)

usual diagnostic plots for constant-pressure tests represent both the inverse flow rate normalized by the pressure and its derivative in a log–log plot (e.g., Fig. 5). This allows avoiding misinterpretations of hydraulic properties using the Jacob & Lohman model in cases where the radial flow assumption or the homogeneous reservoir assumption is not met (Ferroud et al. 2019). Second, the generalized radial flow (GRF) model and its extension to dual-porosity medium have generalized the interpretation of hydraulic tests to a n dimension, i.e., non radial flow around the well in a fully saturated, homogenous, and isotropic reservoir (Barker 1988). Doe (1991) presented a generalized solution of the GRF model for constant-pressure tests. Usually, this solution is fitted in the Laplace space and the real-space solution is calculated by numerical inversion of the Laplace-transform solution to generate type curves using dedicated software.

Other analytical solutions exist more dedicated to particular cases and less commonly applied (e.g., Gringarten et al. 1974; Ozkan and Raghavan 1991). However, we have not identified any solution adapted to tests in unsaturated medium. Considering that the initial saturation is sufficiently high, we will therefore apply the most common solutions of Jacob and Lohman (1952) and Barker (1988) to the tests and then evaluate the results using numerical modeling. The detailed equations for each solution can be found in the related literature. They have been implemented in different software. For this study, we used the AQTESOLV software (Duffield 2007).

Numerical simulations

The relevancy of analytically estimated properties is checked through a numerical approach. 3D small-scale cylindrical flow models centered on the well interval tested are built in the FEFLOW software (Diersch 2014; Trefry and Muffels 2007). As the radius of investigation of the tests is low, the well radius cannot be neglected and is directly modeled within the grid. Cells located around it are locally refined to catch properly details around the well. Pressure values from the tests data are used as boundary condition.

These models aim at reproducing the injection process, considering the unsaturated nature of the reservoir, to estimate properties numerically and compare with analytical results. To define the relationship between water saturation, relative permeability, and pressure, the empirical model of Van Genuchten (1980) is applied. Two fitting parameters are needed in this model: α (m^{-1}) and n (unit less). These parameters are highly uncertain and have been rarely characterized for carbonate rock (Andriani et al. 2021). Here, we performed a sensitivity analysis around default values taken from the literature (Dal Soglio et al. 2020; Kordilla et al. 2012; Roulier et al. 2006).

In most of the intervals tested, several tests were performed successively (for more details, see Duboeuf 2018; Duboeuf et al. 2017, 2021). To simulate the considered constant-pressure steps, it is important to consider that the reservoir is already saturated around the well due to previous injections. To overcome this issue, injected volume before

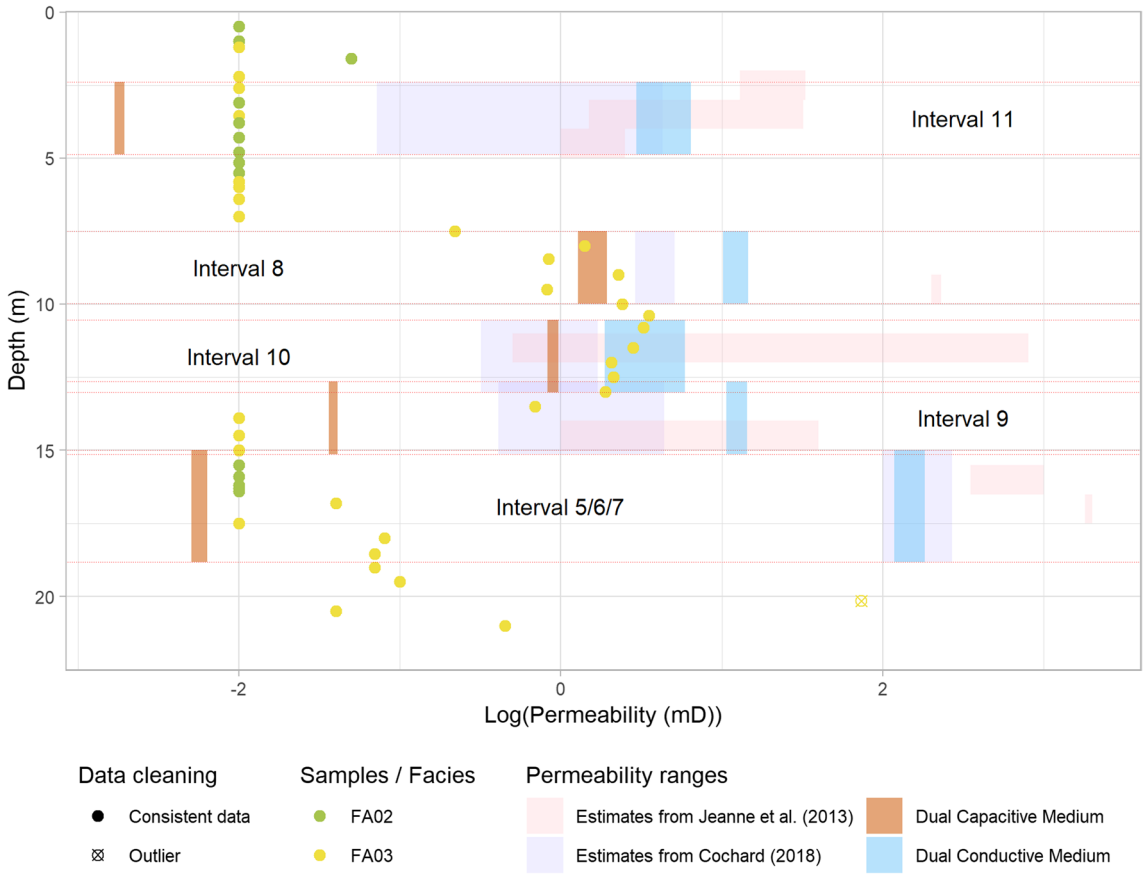

Fig. 6 Comparison of the different permeability values in the P2 borehole, resulting from both small-scale measurements on plugs (points, colored according to the facies, limit of quantification = 10^{-2} mD) and interpretation of injection tests in sealed intervals (rectangles, whose vertical and horizontal extensions correspond respectively to the thickness of the tested interval and the permeability range deduced from the interpretation of the tests in the interval)

the studied test is calculated from the data. This volume is injected in the model before the simulation of the test, to define a consistent initially saturated volume around the well. Before any prior injection, initial saturation in the reservoir is defined at 0.75, as no measurements are available. The use of a high initial water saturation value can be justified by the depth of the well (280 m below the surface) and by the fact that water is constantly dripping in the tunnel gallery, indicating a high saturation.

Porosity is input from plug measurements. Single medium permeability and storage capacity are investigated parameters by trial-and-error process.

Results and discussion

A systematic dual medium behavior at meter scale

Each hydraulic test was analyzed using AQTESOLV software (Duffield 2007). For all hydraulic tests, the log–log diagnostic plot shows both a very short (< 1 s) wellbore storage effect, as expected (Doe 1991; Renard 2005), and a U-shaped derivative (after 1 s), typical of a dual-medium behavior (e.g., Renard et al. 2009), as illustrated in Fig. 5. Thus, Barker's analytical solution for dual-porosity reservoirs provides the best data match. The permeability values obtained from these tests interpretation are presented in Table 1. These values are independent of the small-scale measurements carried out on the plugs with which we will compare them. For the sake of usage and simplicity, the two media characterized by a test are named capacitive medium and conductive medium regardless of their geological characteristics.

For all the tests and intervals, the permeability of the capacitive medium varies between $7e^{-4}$ mD and 2 mD, the permeability of the conductive medium, between 2 and 300 mD. Since all tests were performed in a volume of a few cubic meters (P2 and P5 are 5 m apart) and within only two facies associations, FA2 and FA3, these ranges of values give an idea of the large spatial variability of permeability in fractured and karstified carbonates. Figure 6 compares the permeability ranges for the set of tests processed per

tested interval of well P2 to the previous estimates from the literature (Cochard 2018; Jeanne et al. 2013) and the small-scale measurements on plugs from Cochard (2018). The latter range from less than 0.01 mD (limit of quantification) to 3.54 mD.

In general, Fig. 6 shows less spread out permeability ranges for the dual-medium interpretation than for the roughly estimated values from the previous studies, considering a single average equivalent permeability of the whole medium. This representation with an average permeability appears to be essentially controlled by fracture permeability when matrix permeability is low, as shown for intervals 11 and 5–7 in Fig. 6. However, interval 8 (P2) for instance, whose permeability of the capacitive medium is both relatively high (1.7 mD on average) and not very different from the permeability of the conductive medium (13.5 mD on average), illustrates different weights in the contribution of each medium to obtain the single equivalent permeability. It is therefore difficult to relate geological characteristics to a single medium permeability value estimated for a medium with multi-medium behavior.

Despite their proximity, the same lithological facies, the same texture, and small-scale permeability values of the same order of magnitude, the permeability values from hydraulic tests' interpretation are different in intervals 8 and 10 (Fig. 6). On the one hand, the results of interval 8 show a capacitive medium permeability (1.7 mD on average) of the same order of magnitude as the plugs' measurements (1.1 mD on average) and a conductive medium permeability of an order of magnitude higher (13.5 mD on average). On the other hand, the results of interval 10 show a conductive medium permeability (3.6 mD on average) of the same order of magnitude as the plugs measurements (3.05 mD on average) and a lower capacitive medium permeability (0.9 mD on average). In the case of a dual-medium interpretation, the studied medium behaves as two media of different capacity and conductivity, nested and exchanging between them. In most cases, these correspond to a matrix continuum of low permeability and more conductive fractures or karst conduits, which leads to the often abusive naming of the two media matrix and fractures or matrix and conduits. In the present case, almost no discontinuities were observed on interval 10 and a few discontinuities (Fig. 3) with a maximum aperture of 1.5 mm (Fig. 7) were observed on interval 8. Multi-centimeter cemented fossils of rudists are present in the two intervals (Fig. 4a, b), and purposely avoided during sampling. These cemented impermeable elements could induce this dual-medium response with a lower permeability in interval 10. The presence of fine conductive discontinuities in interval 8 hides this behavior. Indeed, the fractured and karstified carbonate medium investigated is a complex multi-medium with a multi-scale heterogeneity whose dual-medium interpretation of hydraulic tests only identifies the two main end-members.

Permeability according to the geological features

The intervals 3 (P5), and 8 and 10 (P2) are characterized by rudist-rich facies (FA3) only and mostly floatstone (> 96%) with very few, poorly open (< 1.5 mm) discontinuities. They have a capacitive medium permeability, around 2 mD according to plug measurements and ranging from 0.2 to 2 mD according to test interpretation. These values are relatively high compared to measurements made on other

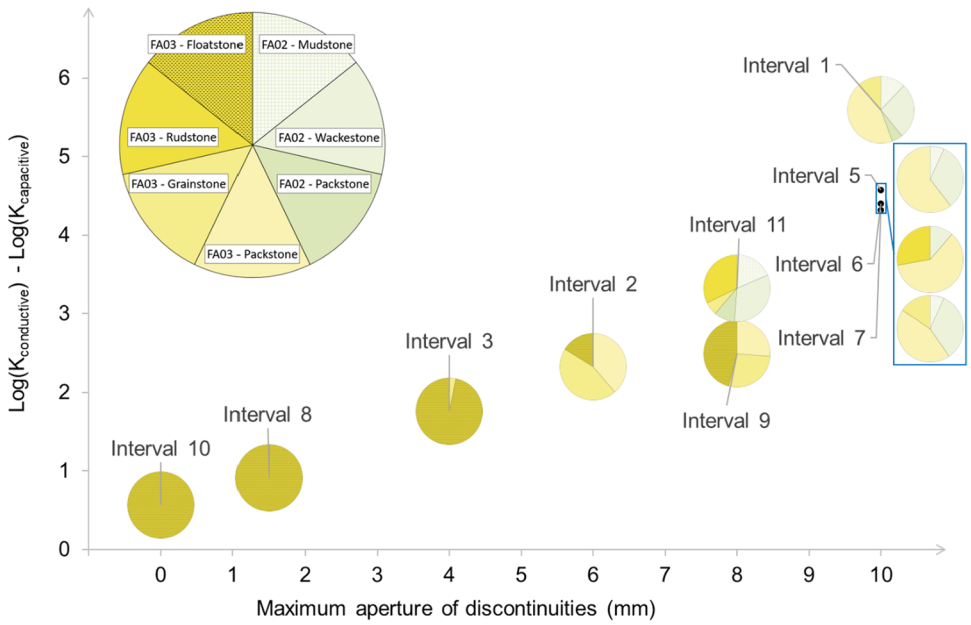

Fig. 7 Dual medium average contrast of permeability as a function of discontinuities maximum aperture, also considering the facies and textures proportions in the tested intervals

lithologies. The conductive medium permeability is not very contrasting compared to the matrix permeability, ranging from 2 to 16 mD (Table 1 and Fig. 6).

On the other hand, the intervals 1 (P5), 5–7 and 11 (P2), which are composed of both FA2 and FA3 facies in various proportions, have the highest proportions of mudstone-to-packstone textures. They exhibit both the lowest permeability for the capacitive medium (< 6e−3mD) and the highest permeability for the conductive medium [up to 300 mD for interval 1 (P5)], thus the greatest permeability contrast as highlighted in Fig. 7. This is consistent with the high density and large aperture of discontinuities observed in these intervals.

The dual-medium permeability contrast has been calculated for each test and the average was calculated for each interval. It was thus compared to the maximum aperture of the discontinuities observed in the tested intervals, also considering the facies and textures proportions (Fig. 7). It confirmed a strong and expected correlation between the permeability contrast and the aperture of discontinuities ($R = 0.94$), which is itself more correlated with the texture of the rock ($R = 0.91$ considering the proportion of textures between mudstone and packstone) than with the sedimentary facies ($R = 0.64$).

Permeability according to the scale

As described previously for intervals 8 and 10, most of the permeability values from plug measurements are consistent with the capacitive medium permeability from the tests. Indeed, the values are of the same order of magnitude, or the differences have been explained according to the geological characteristics. This validates, in this case at least, the often-questioned representativeness of small-scale measurements. Furthermore, quantifying the differences between the permeability values evaluated at different scales and relating these differences to the characteristics and heterogeneity of the sampled volumes are keys to addressing the upscaling issue.

The sampling methodology for laboratory measurements aims to take homogeneous, one-piece samples that are representative of the rock under consideration, especially from a sedimentological point of view. Heterogeneity larger than the volume of the plug, such as fractures or large cemented fossils, is therefore deliberately avoided (e.g., Fig. 4). Note that micro-fractures, which may be missed or occur during sampling, result in an outlier high permeability value, as in P2 at 20.15 m depth (Fig. 6). Conversely, possible sample-wide impermeable elements would lead to very low and unrepresentative permeability values, nevertheless more difficult to identify as outliers. The permeability values obtained from laboratory measurements are ultimately only representative of the sampled porous medium. Their use in an upscaling process is therefore useful but is only relevant in connection with a precise description of this medium.

Hydraulic tests involve larger volumes, whose shape is nevertheless difficult to estimate, between cylindrical and spherical, with a deeper penetration in preferential flow paths such as open discontinuities. In the present case, the sealed interval sets a minimum thickness of 2.48 m and, given the estimated porosity, the injected volumes, calculated from flow measurements (e.g., Fig. 8), make it possible to roughly estimate investigation radii of the order of a few decimeters to a few meters, with an uncertainty that is therefore all the greater as the duality of the recorded behavior is marked. As a first consequence, the hydraulic tests seem to have a lower limit of quantification than the small-scale measurements. Interpretation of some of the tests yields permeability values of the order of $1e^{-3}$ mD, lower than

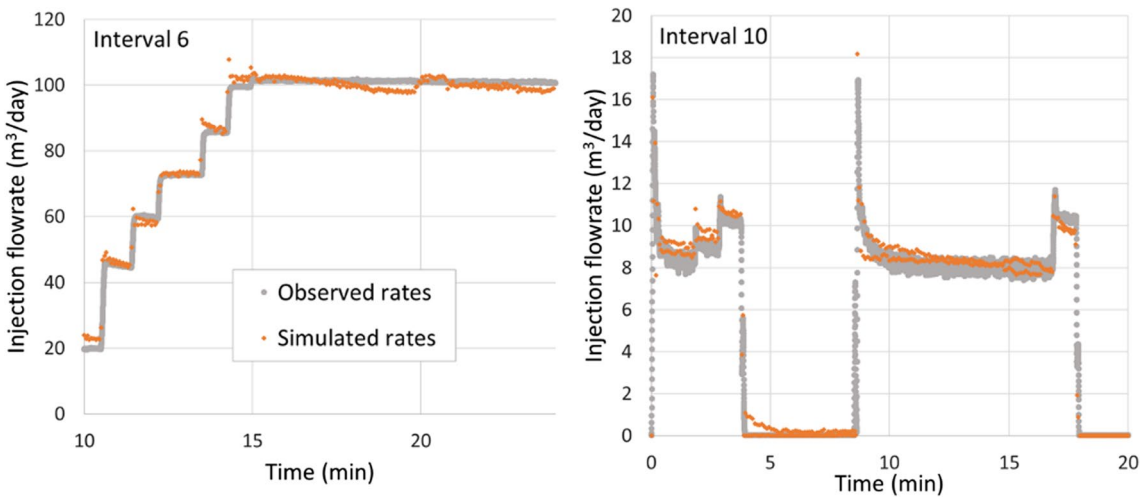

Fig. 8 Simulation results compared to data for successive tests in interval 6 and interval 10

the limit of quantification ($1e^{-2}$ mD) of laboratory measurements, reached for several plugs (Fig. 6). Indeed, for a given measurement uncertainty, the larger the volumes and discharges, the lower the limit of quantification. However, the impact is probably very small at this very low level of permeability.

As a second consequence, the heterogeneity not accounted for by small-scale measurements affects the hydraulic tests. Here, the description of the plugs (e.g., facies in Fig. 6) and tested intervals (Figs. 3, 7) helped to explain the differences between the permeability values at different scales and from one interval to another. However, is it possible to give indications of permeability on other or larger volumes than those explored from this knowledge? For similar facies, textures, and discontinuities in a volume of the same order of magnitude, this is certainly possible from the relationship shown in Fig. 7. For other configurations, the interdisciplinary methodology presented could be adapted. However, the systematically observed dual-medium behavior also highlights the larger scale heterogeneity that remains unaccounted for by the meter scale tests. Indeed, the dual-medium behavior highlights the impact of heterogeneity, which size is larger than the volume studied. Otherwise, the volume of rock studied would be equivalent to a homogeneous medium and a single medium solution would allow the interpretation of the tests. This points out the multi-scale heterogeneity of carbonates and the delicate definition of an elementary volume representative of these media, yet essential for upscaling properties.

Insights from numerical simulations

Figure 8 shows the match between the injection rates from the simulation results and the data, for interval 10 and interval 6. Interval 10 only targets floatstone rudist facies (FA3) with almost no discontinuities observed. Conversely, interval 6 consists of the two facies and different textures ranging from wackestone to rudstone. It is also and primarily marked by several stratigraphic and tectonic discontinuities, some with centimeter aperture due to karstification.

For interval 10, the best match for simulation of several tests in a row is obtained for a permeability of 3 mD. This value is of the same order of magnitude as the permeability values deduced from the analytical interpretation, between 2 and 6 mD for the conductive medium, close to 1 mD for the capacitive medium (Table 1 and Fig. 6). In this case, in agreement with the geological description, the permeability contrast of the dual medium is small. The approximation of saturated simple medium made in the numerical simulations does not prevent the calibration of the model.

For interval 6, a permeability increasing with time, from 92 to 109 mD, is necessary to obtain the best fit for the simulation of several tests in a row. This evolution with time is a proxy for the evolution of the equivalent permeability of the increasing saturated volume explored by the tests. It highlights the variability in permeability that may be due to the increase in saturation of the medium and/or an increase in permeability away from the well. Besides, the variability observed in the analytical interpretation of test series (Fig. 6, horizontal extension of the rectangles) can have the same explanation. Here, due to largely open discontinuities, the permeability contrast is high and the dual medium behavior is likely important to consider, which makes the assumptions made for numerical simulations debatable. Moreover, the shape of the volume explored by the test is probably complex, with water flowing far away from the borehole through open discontinuities. The evolution of permeability needed is nevertheless small and the values are of the same order of magnitude as the permeability of the conductive medium according to the analytical interpretation (126 mD, Table 1).

Finally, the values obtained analytically by applying solutions adapted to the saturated medium are consistent with the calibration values of a simulation in unsaturated medium.

Conclusion

The purpose of this study was to investigate the variability of permeability in limestone for rarely studied sub-meter scales. Rather than looking for a relationship only between permeability and scale, as the power-law functions existing in the literature (e.g., Matheron 1967; Mourlanette et al. 2020; Noetinger 1994), we sought here to relate permeability to the geological characteristics of the studied medium as a function of scale. For this purpose, the study drew on a large body of previously acquired data, combining a comprehensive geological characterization of the medium (facies, texture, and discontinuities), petrophysical measurements on centimeter scale samples, and constant-pressure tests between packers on meter scale.

Assessing permeability at various scales in different neighboring limestone volumes highlights the variability of permeability both in space and from one scale to another, a consequence of the great heterogeneity of this type of medium. The need to consider a dual medium comes into play as early as the meter scale. This demonstrates the multi-scale heterogeneity of carbonate rocks from the smallest scales, and not only when it comes to integrating large structural or karstic elements. This calls therefore into question the possibility of extrapolating usual measurements to larger volumes without additional information, for example from geology.

Quantifying several relationships between matrix and discontinuities features regarding permeability values and permeability contrasts enables characterizing the dual-medium behavior. Furthermore, while the processes leading to the

preferential occurrence of discontinuities in fine-textured limestone have been described in the literature (e.g., Barbier et al. 2012; Gross et al. 1995), this work quantifies their consequence in terms of permeability and hydraulic behavior. In particular, fine-textured facies show a more pronounced dual hydraulic behavior than more granular facies.

Finally, from the scale of cemented centimeter fossils acting as barriers to the scale of wide-open discontinuities favoring the flow, this study has shown that the karst environment is a complex multi-medium with multi-scale heterogeneity even at the smallest scales. Evaluating permeability at different intermediate scales by relating it to geological features seems to be a right way to understand this heterogeneity and to determine correctly the permeability at the desired scale.

Acknowledgements The authors would like to thank TotalEnergies for funding the ALBION R&D project**,** of which this study is a part, and for giving permission to publish this paper.

Author contributions C.D. and G.M. designed the study. J.C. performed the analytical interpretations and numerical simulations of the hydraulic tests, with the assistance of M.B. and L.D.S., and the guidance of C.D., G.M., and J.L.L. P.L. and M.B. provided, reviewed, and improved the geologic descriptions from previous studies. C.D. performed the joint interpretation of the data and wrote the manuscript. G.M. and J.L.L. supervised and obtained financial support for the project leading to this publication. All authors commented on previous versions of the manuscript, read and approved the final manuscript.

Data availability Not applicable.

Declarations

Competing interests The authors declare no competing interests.

References

Andriani GF, Pastore N, Giasi CI, Parise M (2021) Hydraulic properties of unsaturated calcarenites by means of a new integrated approach. J Hydrol 602:15. https://doi.org/10.1016/j.jhydrol.2021.126730

Barbier M, Hamon Y, Callot JP, Floquet M, Daniel JM (2012) Sedimentary and diagenetic controls on the multiscale fracturing pattern of a carbonate reservoir: the Madison Formation (Sheep Mountain, Wyoming, USA). Mar Pet Geol 29:50–67. https://doi.org/10.1016/j.marpetgeo.2011.08.009

Barbier M, Léonide P, Lanteaume C, Borgomano J, Massonnat G (2021) Quantitative sequence stratigraphy applied to the Barremian/Lower Aptian Urgonian carbonate platform (Provence, France). In: Babek O, Stanislava V (eds) 35th IAS meeting of sedimentology. Palacky University Olomouc, Prague

Barker JA (1988) A generalized radial flow model for hydraulic tests in fractured rock. Water Resour Res 24:1796–1804. https://doi.org/10.1029/WR024i010p01796

Blavoux B, Mudry J, Puig JM (1992) The Karst system of the Fontaine de Vaucluse (Southeastern France). Environ Geol Water Sci 19:215–225. https://doi.org/10.1007/bf01704088

Blondel T, Emblanch C, Batiot-Guilhe C, Dudal Y, Boyer D (2012) Punctual and continuous estimation of transit time from dissolved organic matter fluorescence properties in karst aquifers, application to groundwaters of 'Fontaine de Vaucluse' experimental basin (SE France). Environ Earth Sci 65:2299–2309. https://doi.org/10.1007/s12665-012-1562-x

Bonacci O (2007) Analysis of long-term (1878–2004) mean annual discharges of the karst spring Fontaine de Vaucluse (France). Acta Carsologica 36:151–156. https://doi.org/10.3986/ac.v36i1.217

Bonnet M, Margat J, Thiéry D (1976) Essai de représentation du comportement hydraulique d'un système karstique par modèle déterministe, application à la Fontaine de Vaucluse. Deuxième colloque d'hydrologie en Pays calcaire. Annales Scientifiques de l'Université de Besançon, Besançon, pp 79–95

Borgomano J, Masse JP, Fenerci-Masse M, Fournier F (2013) Petrophysics of lower cretaceous platform carbonate outcrops in Provence (SE France): implications for carbonate reservoir characterization. J Pet Geol 36:5–41. https://doi.org/10.1111/jpg.12540

Bourdet D, Whittle T, Douglas A, Pirard Y (1983) A new set of type curves simplifies well test analysis. World Oil 196:95–106

Brunetti C, Bianchi M, Pirot G, Linde N (2019) Hydrogeological model selection among complex spatial priors. Water Resour Res 55:6729–6753. https://doi.org/10.1029/2019wr024840

Carriere SD, Chalikakis K, Danquigny C, Davi H, Mazzilli N, Ollivier C, Emblanch C (2016) The role of porous matrix in water flow regulation within a karst unsaturated zone: an integrated hydrogeophysical approach. Hydrogeol J 24:1905–1918. https://doi.org/10.1007/s10040-016-1425-8

Cochard J (2018) Analyses des propriétés réservoirs d'une série carbonatée microporeuse fracturée: approches multi-échelle sédimentologiques, diagénétiques etmécaniques intégrées. PhD Thesis, Aix-Marseille University, France

Cochard J, Léonide P, Borgomano J, Guglielmi Y, Massonnat G, Rolando J-P, Marié L, Pasquier A (2020) Reservoir properties of Barremian–Aptian Urgonian limestones, SE France, part 1: influence of structural history on porosity-permeability variations. J Pet Geol 43:75–94. https://doi.org/10.1111/jpg.12750

Cochard J, Leonide P, Borgomano J, Guglielmi Y, Massonnat G, Rolando JP, Marie L, Pasquier A (2021) Reservoir properties of Barremian-Aptian Urgonian limestones, SE France, part 2: influence of diagenesis and fracturing. J Pet Geol 44:97–113. https://doi.org/10.1111/jpg.12780

Cognard-Plancq A-L, Gevaudan C, Emblanch C (2006) Historical monthly rainfall-runoff database on Fontaine de Vaucluse karst system : review and lessons. In: Duran J-J, Andreo B, Carrasco F (eds) Karst, climate change and groundwater Karst, cambio climatico y aguas submediterraneas. Ministerio de Educacion y Ciencia. Instituto Geológico y Minero de España, Malaga, pp 465–475

Dal Soglio L, Danquigny C, Massonnat G, Mazzilli N, Emblanch C (2019) New insights into karst genesis processes in unsaturated zone thanks to process-like modelling. In: 46th IAH Congress, Malaga, p 424

Dal Soglio L, Danquigny C, Mazzilli N, Emblanch C, Massonnat G (2020) Modeling the matrix-conduit exchanges in both the epikarst and the transmission zone of karst systems. Water 12:19. https://doi.org/10.3390/w12113219

Danquigny C, Massonnat G, Mermoud C, Rolando J-P (2019a) Intra- and inter-facies variability of multi-physics data in carbonates. New insights from database of ALBION R&D Project. Abu Dhabi international petroleum exhibition & conference. Society of Petroleum Engineers, Abu Dhabi, p 11. https://doi.org/10.2118/197836-MS

Danquigny C, Massonnat G, Tendil A, Dal Soglio L, Cochard J, Dumont I, Mazzilli N, Emblanch C, Chalikakis K, Léonide P, Borgomano J, Fournier F, Sénéchal G, Rousset D, Garambois S, Voisin C, Brito D, Rebelle M, Rolando J-P (2019b) Inter-disciplinary characterization of carbonate reservoirs. ALBION, a multi-scales dynamic analogue. In: 46th IAH Congress, Malaga, p 422

Danquigny C, Massonnat G, Barbier M, Bouxin P, Dal Soglio L, Lesueur J-L (2021) Contribution of the ALBION dynamic analogue in understanding the diversity of fluid flows in fractured carbonate reservoirs. The Example of the LSBB Instrumented Site. Abu Dhabi International Petroleum Exhibition & Conference, Abu Dhabi. https://doi.org/10.2118/207664-ms

Danquigny C, Coqueret J, Massonnat G, Leonide P, Barbier M, Dal Soglio L, Lesueur J-L (2023) A smart analytical and numerical interpretation of injection tests in unsaturated, fractured and karstified carbonate reservoirs. In: Bartolomé A, Barberá JA, Durán JJ, Gil-Márquez JM, Mudarra M (eds) EuroKarst 2022, Málaga advances in the hydrogeology of karst and carbonate reservoirs. Springer Nature Switzerland AG, p 8

Diersch H-J (2014) FEFLOW. Finite element modeling of flow, mass and heat transport in porous and fractured media. Springer, Berlin

Doe TW (1991) Fractional dimension analysis of constant-pressure well tests. In: SPE annual technical conference and exhibition. https://doi.org/10.2118/22702-ms

Duboeuf L (2018) Injections de fluide dans une zone de faille (LSBB, Rustrel): sismicité induite et déformation asismique. PhD Thesis, Université Côte d'Azur, Nice

Duboeuf L, De Barros L, Cappa F, Guglielmi Y, Deschamps A, Seguy S (2017) Aseismic motions drive a sparse seismicity during fluid injections into a fractured zone in a carbonate reservoir. J Geophys Res-Solid Earth 122:8285–8304. https://doi.org/10.1002/2017jb014535

Duboeuf L, De Barros L, Kakurina M, Guglielmi Y, Cappa F, Valley B (2021) Aseismic deformations perturb the stress state and trigger induced seismicity during injection experiments. Geophys J Int 224:1465–1476. https://doi.org/10.1093/gji/ggaa515

Duffield GM (2007) AQTESOLV for Windows version 4.5 user's guide. Reston, Virginia

Emblanch C, Zuppi GM, Mudry J, Blavoux B, Batiot C (2003) Carbon 13 of TDIC to quantify the role of the unsaturated zone: the example of the Vaucluse karst systems (Southeastern France). J Hydrol 279:262–274. https://doi.org/10.1016/S0022-1694(03)00180-X

Enemark T, Peeters LJM, Mallants D, Batelaan O (2019) Hydrogeological conceptual model building and testing: a review. J Hydrol 569:310–329. https://doi.org/10.1016/j.jhydrol.2018.12.007

Ferroud A, Rafini S, Chesnaux R (2019) Using flow dimension sequences to interpret non-uniform aquifers with constant-rate pumping-tests: a review. J Hydrol X 2:25. https://doi.org/10.1016/j.hydroa.2018.100003

Fleury P, Plagnes V, Bakalowicz M (2007) Modelling of the functioning of karst aquifers with a reservoir model: application to Fontaine de Vaucluse (South of France). J Hydrol 345:38–49. https://doi.org/10.1016/j.jhydrol.2007.07.014

Ford DC, Williams PW (2007) Karst hydrogeology and geomorphology. Wiley, Chichester

Galvao P, Halihan T, Hirata R (2016) The karst permeability scale effect of Sete Lagoas, MG, Brazil. J Hydrol 532:149–162. https://doi.org/10.1016/j.jhydrol.2015.11.026

Geier JE, Benabderrahman A, Haessler L, Doe TW (1996) Generalized radial flow interpretation of well tests for the SITE-94 project. Swedish Nuclear Power Inspectorate, Stockholm, p 184

Ghasemizadeh R, Hellweger F, Butscher C, Padilla I, Vesper D, Field M, Alshawabkeh A (2012) Review: Groundwater flow and transport modeling of karst aquifers, with particular reference to the North Coast Limestone aquifer system of Puerto Rico. Hydrogeol J 20:1441–1461. https://doi.org/10.1007/s10040-012-0897-4

Gringarten AC, Ramey HJ Jr, Raghavan R (1974) Unsteady-state pressure distributions created by a well with a single infinite-conductivity vertical fracture. Soc Petrol Eng J 14:347–360. https://doi.org/10.2118/4051-pa

Gross MR, Fischer MP, Engelder T, Greenfield RJ (1995) Factors controlling joint spacing in interbedded sedimentary rocks: integrating numerical models with field observations from the Monterey Formation, USA. Geol Soc Lond Spec Publ 92:215–233. https://doi.org/10.1144/GSL.SP.1995.092.01.12

Halihan T, Sharp JM, Mace RE (1999) Interpreting flow using permeability at multiple scales. In: Palmer AN, Palmer MV, Sasowsky ID (eds) Karst modeling: special publication 5. The Karst Waters Institute, pp 82–96

Hantush MS (1959) Nonsteady flow to flowing wells in leaky aquifers. J Geophys Res 1896–1977(64):1043–1052. https://doi.org/10.1029/JZ064i008p01043

Hartmann A, Goldscheider N, Wagener T, Lange J, Weiler M (2014) Karst water resources in a changing world: Review of hydrological modeling approaches. Rev Geophys 52:218–242. https://doi.org/10.1002/2013rg000443

Jacob CE, Lohman SW (1952) Nonsteady flow to a well of constant drawdown in an extensive aquifer. EOS Trans Am Geophys Union 33:559–569. https://doi.org/10.1029/TR033i004p00559

Jazayeri Noushabadi MR, Jourde H, Massonnat G (2011) Influence of the observation scale on permeability estimation at local and regional scales through well tests in a fractured and karstic aquifer (Lez aquifer, Southern France). J Hydrol 403:321–336. https://doi.org/10.1016/j.jhydrol.2011.04.013

Jeanne P, Guglielmi Y, Cappa F (2013) Dissimilar properties within a carbonate-reservoir's small fault zone, and their impact on the pressurization and leakage associated with CO_2 injection. J Struct Geol 47:25–35. https://doi.org/10.1016/j.jsg.2012.10.010

Kordilla J, Sauter M, Reimann T, Geyer T (2012) Simulation of saturated and unsaturated flow in karst systems at catchment scale using a double continuum approach. Hydrol Earth Syst Sci 16:3909–3923. https://doi.org/10.5194/hess-16-3909-2012

Leonide P, Borgomano J, Masse JP, Doublet S (2012) Relation between stratigraphic architecture and multi-scale heterogeneities in carbonate platforms: the Barremian-lower Aptian of the Monts de Vaucluse, SE France. Sediment Geol 265:87–109. https://doi.org/10.1016/j.sedgeo.2012.03.019

Leonide P, Fournier F, Reijmer JJG, Vonhof H, Borgomano J, Dijk J, Rosenthal M, van Goethem M, Cochard J, Meulenaars K (2014) Diagenetic patterns and pore space distribution along a platform to outer-shelf transect (Urgonian limestone, Barremian-Aptian, SE France). Sediment Geol 306:1–23. https://doi.org/10.1016/j.sedgeo.2014.03.001

Linde N, Renard P, Mukerji T, Caers J (2015) Geological realism in hydrogeological and geophysical inverse modeling: a review. Adv Water Resour 86:86–101. https://doi.org/10.1016/j.advwatres.2015.09.019

Linde N, Ginsbourger D, Irving J, Nobile F, Doucet A (2017) On uncertainty quantification in hydrogeology and hydrogeophysics.

Adv Water Resour 110:166–181. https://doi.org/10.1016/j.advwatres.2017.10.014
Marechal JC, Ladouche B, Dorfliger N, Lachassagne P (2008) Interpretation of pumping tests in a mixed flow karst system. Water Resour Res 44:18. https://doi.org/10.1029/2007wr006288
Maréchal J-C, Ladouche B, Dewandel B, Fleury P, Dörfliger N (2014) Diagnostic plots applied to well-tests in karst systems. In: Mudry J, Zwahlen F, Bertrand C, LaMoreaux JW (eds) H2Karst research in limestone hydrogeology. Springer International Publishing, Cham, pp 127–137
Masse JP (1967) L'Urgonien de Sault (Vaucluse). Bull Soc Géol Fr S7-IX:495–496. https://doi.org/10.2113/gssgfbull.S7-IX.4.495
Masse J-P (1976) Les calcaires urgoniens de Provence (Valanginien-Aptien inférieur). Stratigraphie, paléontologie, les paléoenvironnements et leur évolution. PhD Thesis, Aix-Marseille II University, France
Massonnat G, Rolando JP, Danquigny C (2017) The ALBION project: an observatory in the heart of a carbonate reservoir. In: Abu Dhabi international petroleum exhibition & conference. Society of Petroleum Engineers, Abu Dhabi, p 9. https://doi.org/10.2118/188539-MS
Massonnat G, Danquigny C, Rolando J-P (2019) Permeability upscaling in carbonates. An integrated case study from the Albion R&D Project. In: Abu Dhabi international petroleum exhibition & conference. Society of Petroleum Engineers, Abu Dhabi, p 8. https://doi.org/10.2118/197122-MS
Matheron G (1967) Eléments pour une théorie des milieux poreux. Masson, Paris
Mazzilli N, Guinot V, Jourde H, Lecoq N, Labat D, Arfib B, Baudement C, Danquigny C, Dal Soglio L, Bertin D (2019) KarstMod: a modelling platform for rainfall—discharge analysis and modelling dedicated to karst systems. Environ Model Softw 122:7. https://doi.org/10.1016/j.envsoft.2017.03.015
Medici G, West LJ (2021) Groundwater flow velocities in karst aquifers; importance of spatial observation scale and hydraulic testing for contaminant transport prediction. Environ Sci Pollut Res 28:43050–43063. https://doi.org/10.1007/s11356-021-14840-3
Mejias M, Renard P, Glenz D (2009) Hydraulic testing of low-permeability formations. A case study in the granite of Cadalso de los Vidrios, Spain. Eng Geol 107:88–97. https://doi.org/10.1016/j.enggeo.2009.05.010
Michel J, Lanteaume C, Massonnat G, Borgomano J, Tendil A, Bastide F, Frau C, Léonide P, Rebelle M, Barbier M, Danquigny C, Rolando JP (2023) Questioning carbonate facies model definition with reference to the Lower Cretaceous Urgonian platform (SE France Basin). BSGF Earth Sci Bull. https://doi.org/10.1051/bsgf/2023009
Mourlanette P, Biver P, Renard P, Noetinger B, Caumon G, Perrier YA (2020) Direct simulation of non-additive properties on unstructured grids. Adv Water Resour 143:14. https://doi.org/10.1016/j.advwatres.2020.103665
Noetinger B (1994) The effective permeabilitty of a heterogeneous porous medium. Transp Porous Media 15:99–127. https://doi.org/10.1007/BF00625512
Ollivier C, Chalikakis K, Mazzilli N, Kazakis N, Lecomte Y, Danquigny C, Emblanch C (2019) Challenges and limitations of karst aquifer vulnerability mapping based on the PaPRIKa method-application to a large european karst aquifer (Fontaine de Vaucluse, France). Environments 6:13. https://doi.org/10.3390/environments6030039
Ollivier C, Mazzilli N, Olioso A, Chalikakis K, Carriere SD, Danquigny C, Emblanch C (2020) Karst recharge-discharge semi distributed model to assess spatial variability of flows. Sci Total Environ 703:20. https://doi.org/10.1016/j.scitotenv.2019.134368
Ozkan E, Raghavan R (1991) New solutions for well-test-analysis problems: part 1-analytical considerations(includes associated papers 28666 and 29213). In: SPE-12777-PA 6, pp 359–368. https://doi.org/10.2118/18615-pa
Renard P (2005) The future of hydraulic tests. Hydrogeol J 13:259–262. https://doi.org/10.1007/s10040-004-0406-5
Renard P, Glenz D, Mejias M (2009) Understanding diagnostic plots for well-test interpretation. Hydrogeol J 17:589–600. https://doi.org/10.1007/s10040-008-0392-0
Roulier S, Baran N, Mouvet C, Stenemo F, Morvan X, Albrechtsen HJ, Clausen L, Jarvis N (2006) Controls on atrazine leaching through a soil-unsaturated fractured limestone sequence at Brevilles, France. J Contam Hydrol 84:81–105. https://doi.org/10.1016/j.jconhyd.2005.12.004
Tendil AJB, Frau C, Leonide P, Fournier F, Borgomano JR, Lanteaume C, Masse JP, Massonnat G, Rolando JP (2018) Platform-to-basin anatomy of a Barremian-Aptian Tethyan carbonate system: new insights into the regional to global factors controlling the stratigraphic architecture of the Urgonian Provence platform (southeast France). Cretac Res 91:382–411. https://doi.org/10.1016/j.cretres.2018.05.002
Trefry MG, Muffels C (2007) Feflow: a finite-element ground water flow and transport modeling tool. Ground Water 45:525–528. https://doi.org/10.1111/j.1745-6584.2007.00358.x
Van Genuchten MT (1980) A closed-form equation for predicting the hydraulic conductivity of unsaturated soils. Soil Sci Soc Am J 44:892–898. https://doi.org/10.2136/sssaj1980.03615995004400050002x